Progress In Electromagnetics Research C, Vol. 9, 119–129, 2009

A SIMPLE STRATEGY FOR LIFE SIGNS DETECTION VIA AN X-BAND EXPERIMENTAL SET-UP

M. D'Urso

Centro Ricerche Giugliano, SELEX Sistemi Integrati SpA
Via Circumvallazione Esterna di Napoli,
zona ASI, Giugliano, I-80014, Italy

G. Leone

Dipartimento di Ingegneria dell'Informazione
Seconda Università degli Studi di Napoli
via Roma 29, Aversa I-81031, Italy

F. Soldovieri

Istituto per il Rilevamento Elettromagnetico dell'Ambiente
Consiglio Nazionale delle Ricerche
Via Diocleziano 328, Napoli 80124, Italy

Abstract—In this paper, a simple and effective method for Through-The-Wall (TTW) life signs detection is introduced and discussed. To this aim, a Continuous Wave (CW) Microwave Transceiver working in X-Band is adopted. The detection procedure is based on the evaluation of correlation function in frequency domain between the measured and model signals. In order to ensure the reliability, proper background removal strategies are introduced. The effectiveness of the proposed approach is shown by processing experimental data collected in a realistic TTW scenario.

1. MOTIVATIONS

The contact-less detection of life signs as breathing and heartbeat activity via radar sensing [1] is a well assessed topic in medical applications [2–4] and is gaining new attention for rescue operations [5–7] and homeland defence and security [8, 9].

Corresponding author: F. Soldovieri (soldovieri.f@irea.cnr.it).

Microwave signals in detecting human vital signs have been applied for detecting human people beings trapped under rubble or snow [5–7]. The proposed solution schemes are interesting and take into account the non-trivial difficulties of the problem in realistic conditions. Rubble, for example, is an attenuating medium because of the presence of metallic grids. Furthermore, it is an inhomogeneous medium, with many local discontinuities which can act as targets, thus, preventing the detector from being able to distinguish between the operator's signal and the one of the survivor. Snow is a homogeneous medium, almost transparent to microwave propagation, when it is dry; for such a scenario, interesting solutions are in [7].

Doppler detection of vital signs has been considered very recently in TTW imaging, where the synergic exploitation of both Doppler detection and imaging of hidden objects [9] is very promising to tackle the necessities of the realistic contexts.

Despite of many examples of successful applications, some advancements are still necessary to overcome the difficulties related to the exploitation of the Doppler techniques in realistic scenarios. The first difficulty is related to body random movements and static clutter that can affect in a significant way the accuracy in detection and even provide false alarms. In [10], for example, demodulation techniques are exploited for body random movement cancellation. The multiple-input, multiple-output (MIMO) technique has been proposed to solve the problem of motion artefacts and the presence of multiple subjects. Another proposed approach is the single-input, multiple-output (SIMO) technique. In [11] and [12], the single and multiple antenna systems and SIMO/MIMO signal processing have been explored to isolate desired radar return signals from multiple subjects.

Advanced signal processing methods are necessary for non-contact vital sign detection especially when it is not possible to reliably separate the sinusoidal components because of the smearing and leakage problems, due also to the limitation in the observation time intervals. In any case most of frequency estimation approaches are based on the fast Fourier transform [2].

The present paper falls within the above framework. Taking advantage from a simple scattering model and by exploiting a properly designed measurement set-up working in X-Band regime, aim of the paper is to introduce a simple and effective strategy to detect vital signs in TTW scenarios.

In particular, a new signal processing technique based on the evaluation of the correlation in the Doppler frequency domain, between the measured signal and the theoretically expected signal, is introduced

and tested with experimental data. Moreover, static clutter mitigation procedures are also introduced to achieve higher sensitivity and accurate results. The developed procedure has been tested with experimental data collected at the Laboratories of SELEX Sistemi Integrati SpA, Rome.

2. EXPERIMENTAL SET-UP

This section is subdivided into two sub-sections. First, we introduce the measurement set-up. In particular, the working frequency, its geometry, the adopted antennas are described. The adopted values of the radiated power are reported. The measurement set-up parameters, i.e., the gain factor, the sampling frequency as well as antenna dimensions are also given.

2.1. Description of the Measurement Set-up

The adopted measurement set-up is composed of a microwave coherent transceiver radiating a 10 GHz monochromatic wave as reported in Figure 1. The receiver detects the in-phase (I) and quadrature (Q) components of the backscattered signal, which can be represented in the I-Q plane as a generic complex phasor, whose amplitude and phase vary with the respiratory movement of the human chest, which is of order of a fraction of wavelength. The adopted frequency provides a trade-off between the increased penetration depth of lower frequencies through walls and the observed increased phase shift due to breathing and/or heartbeat at higher frequencies. In addition, emission at

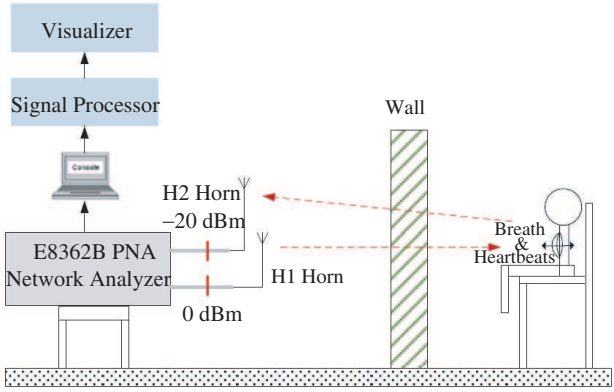

Figure 1. The measurement set-up.

10 GHz does not need a specific license [13]. The two considered sensors are horn antennas, 0 dBm the radiated microwave power, 12 dB the free space antenna gain.

2.2. Details on the Measurements

A transceiver system is used for the synthesis and reception of a monochromatic signal at 10 GHz frequency. The E8362B PNA Network Analyzer, provided by AGILENT, has been employed as transceiver. The equipment is connected to two identical horn antennas in order to transmit and receive the electromagnetic signal, respectively. According to the scheme, the signal is first transmitted by the horn referred to as H_1, reflected by the target and finally received by the H_2 horn.

In the present application, the target is represented by a person and by the wall interposed between the person and the transceiver itself. Therefore, the received base band waveform includes the following contributions: a DC signal due to the wall reflections, two Doppler components associated with the breathing and the heartbeats and, obviously, noise power. With reference to such a kind of the received signal, the main purpose of the signal processor will be to reveal the Doppler components on the noise and DC signal.

After, the backscattered signal is digitally acquired by the equipment for the subsequent processing. A frequency clock equal to 1 kHz and a memory depth equal to 16 KS have been set. Finally, the samples are exchanged to the signal processor and the visualizer. Note that the system needs a proper phase coherent condition, and in the specific case, such a condition is guaranteed by the use of the E8362B PNA as transceiver.

3. THE ADOPTED MATEMATHICAL MODEL

As said above, the problem at hand is concerned with the detection of the vital signs (breathing and heartbeat) and the determination of their frequency for the case of human being beyond an obstacle (i.e., a wall). Though these signals admit a periodic rather involved behavior, we assume the procedure to succeed when the corresponding principal harmonic is detected. Therefore, since this elementary detection scheme is adopted, we do not require to introduce accurate scattering models taking into account all interactions of the electromagnetic field with the objects within the complex scenario at hand. So, since at the chosen operation frequency the body admits very little wave penetration, we adopt the simple model of the electromagnetic

scattering from a sinusoidally vibrating metallic plate [14, 15] located beyond a dielectric slab of thickness d and dielectric permittivity ε_{obs}.

The metallic plate is located at a distance z_0 from the hidden side of the wall. Its varying position is given, within the adopted reference system, by $z(t) = z_0 + A\sin(\omega_d t)$ where A is maximum displacement with respect to the rest position and ω_d is the relevant Doppler frequency.

To compute the field reflected by the vibrating plate, we exploit the quasi-stationarity hypothesis, so that we *freeze* the plate at each time t when it occupies the position z, and compute the scattered field as if the plate is stationary. Accordingly, for a normally impinging plane wave $E_{inc}(z) = E_0 \exp(-jk_0 z)$, where $k_0 = 2\pi/\lambda$ is the wave number, the reflected field is probed at a distance d_{rec} from the first interface of the wall (see Figure 2).

By neglecting the mutual interactions between the plate and the wall, we can assume that the field reflected at $z = -d_{rec}$ can be expressed as

$$E_R(z) = E_0 \exp(-2jk_0 d_{rec})(\Gamma_{wall} + \Gamma_{plate}) \tag{1}$$

where Γ_{wall} is the reflection coefficient (at $z = 0$) due to the obstacle (static clutter) in absence of the plate. In turn, the reflection coefficient due to the plate can be rewritten as

$$\Gamma_{plate} = -T_{wall}^2 \exp(-2jk_0 \hat{z}) \tag{2}$$

where T_{wall} denotes the transmission coefficient through the wall for the normal plane wave incidence. By turning to the Doppler domain,

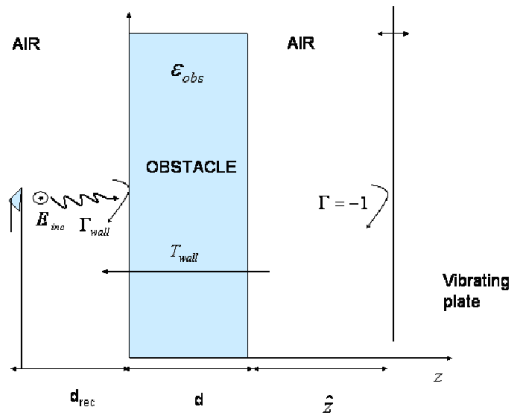

Figure 2. Relevant to the geoemetry of the model.

Equation (1) can be rewritten as

$$E_R(t) = E_{wall} + E_{plate} \exp(-j2k_0 A \sin(\omega_d t)) \tag{3}$$

where

$$E_{wall} = E_0 \Gamma_{wall} \exp(-2jk_0 d_{rec}) \tag{3a}$$

$$E_{plate} = -T_{wall}^2 E_0 \exp(-2jk_0(z_0 + d_{rec})) \tag{3b}$$

These expressions point out the different roles of the wall and the plate. In particular, the first term is related to the reflection of the wall and represents a source for the static clutter. Thus, differently from the free space case, in absence of other static targets, a clutter due to the wall occurs and may overwhelm the searched reflection of the plate. The second term accounts for the field reflected by the plate that undergoes to a transmission in the wall.

This introduces a further difficulty since the amplitude of the desired signal can undergo to an attenuation effect due to the presence of the wall.

4. RECONSTRUCTION SCHEME

The problem at hand is to determine the Doppler frequency ω_d starting from the signal $E_R(t)$ in (3) measured over a finite interval $[0, T]$. The proposed reconstruction procedure is based on three different steps. The first one is concerned with removal/mitigation of the static clutter, i.e., the E_{wall} term in (3) and a successive Fourier transform of the resulting signal so to compute a function $G(\omega_D)$ in Doppler domain.

In the second step, we compute the Fourier Transform of the model signal $\exp[-j2k_0 A \sin(\omega_D t)]$ to obtain

$$E_{model}(\omega_D) = \int_o^T \exp(-2jk_0 A \sin(\omega_D t)) \exp(-j\omega t) dt = \ldots$$

$$\int_o^T \sum_{n=-\infty}^{\infty} J_{-n}(2k_0 A) \exp(jn\omega_D t) \exp(-j\omega t) dt = \ldots$$

$$= \sum_{n=-\infty}^{\infty} J_{-n}(2k_0 A) \sin c[(T/2)(\omega_D - n\omega_D)] \exp(-j(\omega_D - n\omega_D)(T/2)) \tag{4}$$

where we exploit the well know Fourier expansion of the $\exp[-j2k_0 A \sin\ (\omega_D t)]$ term and $J_n(\cdot)$ denotes the Bessel function of first kind and n-th order. Therefore, the Fourier transform of the model signal is made up of a train of sinc functions centred at $n\omega_D$.

Finally, in the third step, the unknown actual principal Doppler frequency ω_d is determined as the quantity that maximizes the scalar product between the square modulus of the *measured* (and preprocessed) Fourier transform $|G(\omega_D)|^2$ and the square modulus of the Fourier transform of the model signal $|E_{model}(\omega_D)|^2$.

It is worth noting that in the proposed procedure the maximum displacement A [see Equation (3)] of the vibration is still unknown. In principle, such a quantity could be determined along the Doppler frequency by maximizing the scalar product. Here, to make the procedure fast so to deal with realistic applications, we assume for the model an estimate of the maximum displacement as $A = 0.5\,\text{cm}$ for the breathing and $A = 1\,\text{mm}$ for the heartbeat.

Finally, it has to be pointed out that the accuracy of the overall procedure is strongly affected by the removal of the static clutter so to obtain a reliable function $G(\omega_D)$ from the experimental data. The ideal clutter removal strategy would be based on the difference between the actual signal and the one when no vital signs are present (background signal). Since such a background measurement is not available at all, in this paper we adopt two alternative strategies.

In the first more common approach, we compute the mean value E_{mean} of the signal over the observation domain $[0, T]$; then we subtract it from the measured one $E_R(t)$ to achieve $\hat{E}_R(t) = E_R(t) - E_{mean}$, so that $G(\omega_D)$ in the subsequent processing is computed from $\hat{E}_R(t)$.

In the second strategy, before applying the same correlation procedure as above, the low-harmonic Doppler content is filtered-out by properly differentiating the measured signal. This can be numerically approximated by subtracting to each measured sample, the previous one.

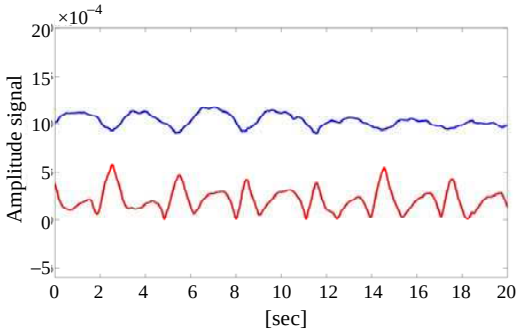

Figure 3. Amplitude of the measured signal $E_R(t)$ (blue line) and of the signal $\hat{E}_R(t)$ after the mean operation (red line) for the first experiment.

5. EXPERIMENTAL RESULTS

This Section reports the results of two experiments of breathing/heartbeat detection and characterization in the TTW configuration. The considered realistic scenario consists of a sitting person inside a furnished room.

The amplitude of the measured signal concerning the first experiment is reported in Figure 3, for $T = 20\,\mathrm{s}$, together with the amplitude of the signal after that the mean operation (first clutter removal strategy) is performed.

Figure 4 depicts the normalized scalar product for different Doppler frequencies. As can be seen, the correlation is peaked around the correct value of 20 events (breaths)/min (i.e., around 0.33 Hz).

The result is achieved by performing the correlation within the Doppler frequency range $f_D = \omega_D/(2\pi) \in [0.08, 0.5]\,\mathrm{Hz}$ with a step of 0.01 Hz. For such a figure and the similar ones reported below, the blue and red lines depict the normalized scalar product starting from the signal where the clutter has been mitigated by the *mean*

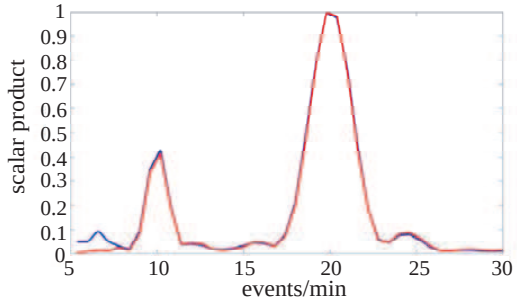

Figure 4. Normalized scalar product versus the number of breathing events per minutes. First experiment.

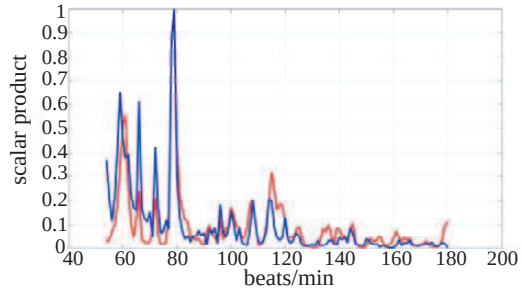

Figure 5. Normalized scalar product versus the number of heartbeats events per minutes. First experiment.

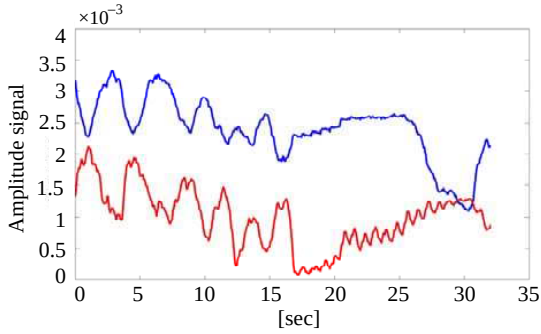

Figure 6. Amplitude of the measured signal $E_R(t)$ (blue line) and of the signal $\hat{E}_R(t)$ after the mean operation (red line) for the second experiment.

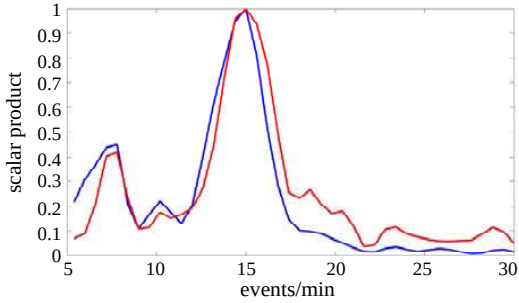

Figure 7. Normalized scalar product versus the number of breathing events per minutes. Second experiment.

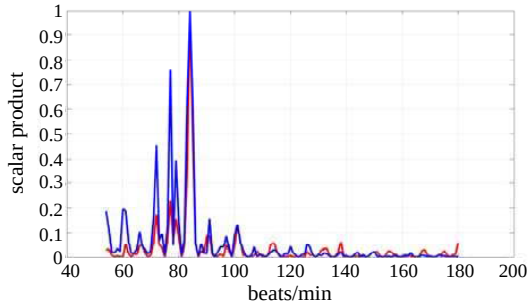

Figure 8. Normalized scalar product versus the number of heartbeats events per minutes. Second experiment.

and *derivative* based procedures, respectively. Then, we perform the heartbeat characterization by searching for the Doppler frequency within the range $[0.9, 3]$ Hz. In this case, see Figure 5, we obtain the maximum of the scalar product for the value of 78 heartbeats/min.

In the second example, during the observation interval, a sequence of breathing and apnoea occurs, see Figure 6.

By performing the same analysis as above we are able to separately appreciate the breathing and heartbeat frequency. In particular, Figure 7 depicts the comparison between the results achieved by the adoption of the different static clutter mitigation strategies. As it can be seen, both the correlations peak at the same value of $f_D = 0.25$ Hz, leading to breaths/min $= 15$.

The same behavior is observed for the heartbeat, see the normalized scalar product in Figure 8, where both the scalar product peaks arises at about heartbeats/min $= 83$.

6. CONCLUSIONS

Life sign detection by microwave Doppler measurements can provide valuable information in many security and rescue applications. In this paper we have applied simple processing strategies to experimental data collected in a realistic scenario (a person beyond a concrete wall and inside a furnished room) by a VNA. After removing the static clutter contribution, we have introduced and applied an algorithm based on the processing of square amplitude of the data Fourier transform (Doppler domain). The comparison with a model signal by correlation provides successfull detection and characterization of both breathing and heart-beat.

ACKNOWLEDGMENT

The authors would like to thank Dr. L. Infante, Dr. R. Lalli and Ing. F. Gianota for having provided the measurements.

REFERENCES

1. Li, C., J. Cummings, J. Lam, E. Graves, and W. Wu, "Radar remote monitoring of vital signs," *IEEE Microwave Magazine*, Vol. 10, 47–56, 2009.
2. Lohman, B., O. Boric-Lubecke, V. M. Lubecke, P. W. Ong, and M. M. Sondhi, "A digital signal processor for Doppler radar sensing of vital signs," *IEEE Engineering in Medicine and Biology*, Vol. 21, 161–164, 2002.

3. Lin, J. C., "Microwave noninvasive sensing of physiological signatures," *Electromagnetic Interaction with Biological Systems*, J. C. Lin (ed.), 3–25, Plenum, New York, 1989.
4. Lin, J. C., "Microwave sensing of physiological movement and volume change: A review," *Bioelectromagnetics*, Vol. 13, 557–565, 1992.
5. Chen, K. M., Y. Huang, J. Zhang, and A. Norman, "Microwave life-detection systems for searching human subjects under earthquake rubble and behind barrier," *IEEE Trans. Biomed. Eng.*, Vol. 27, 105–114, 2000.
6. Arai, I., "Survivor search radar system for persons trapped under earthquake rubble," *Proc. of APMC2001, Taiwan*, 663–667, 2001.
7. Pieraccini, M., G. Luzi, D. Dei, L. Pieri, and C. Atzeni, "Detection of breathing and heartbeat through snow using a microwave transceiver," *IEEE Geoscience and Remote Sensing Letters*, Vol. 5, Vol. 1, 57–59, 2008.
8. Ivashov, S. I., V. Razevig, A. Sheyko, and I. Vasileyev, "Detection of human breathing and heartbeat by remote radar," *PIERS Proceedings*, 663–666, Pisa, Italy, March 28–31, 2004.
9. Lubecke, V. M., O. Boric-Lubecke, A. Host-Madsen, and A. E. Fathy, "Through-the-wall radar life detection and monitoring," *Proc. of Microwave Symposium 2007*, 769–772, 2007.
10. Li, C. and J. Lin, "Random body movement cancellation in Doppler radar vital sign detection," *IEEE Trans. on Microw. Th. Techn.*, Vol. 56, 3143–3152, 2008.
11. Zhou, Q., J. Liu, A. Host-Madsen, O. Boric-Lubecke, and V. Lubecke, "Detection of multiple heartbeats using Doppler radar," *Proc. IEEE ICASSP 2006*, 1160–1163, 2006.
12. Boric-Lubecke, O., V. Lubecke, A. Host-Madsen, D. Samardzija, and K. Cheung, "Doppler radar sensing of multiple subjects in single and multiple antenna systems," *Proc. 7th Int. Conf. on Telecommunication in Modern Satellite, Cable and Broadcasting Services*, 7–11, 2005.
13. [Online] Available at: http//www.icnirp.de.
14. Van Bladel, J. and D. Zutter, "Reflections from linearly vibrating objects: Plane mirror at normal incidence," *IEEE Trans. Antennas Propagat.*, Vol. 29, 629–637, 1981.
15. Ho, M., "One-dimensional simulation of reflected em pulses from objects vibrating at different frequencies," *Progress In Electromagnetics Research*, PIER 53, 239–248, 2005.